Control Engineering Practice 56 (2016) 86–91

Contents lists available at ScienceDirect

Control Engineering Practice

journal homepage: www.elsevier.com/locate/conengprac

Feedforward based transient control in solid oxide fuel cells

Omid Madani [a], Tuhin Das [b,*]

[a] University of Central Florida, Orlando, FL, United States
[b] Mech. & Aero. Engg. Department, University of Central Florida Orlando, FL 32816, United States

ARTICLE INFO

Article history:
Received 9 November 2015
Received in revised form
12 August 2016
Accepted 13 August 2016
Available online 24 August 2016

Keywords:
Solid oxide fuel cell
Fuel utilization
Transient control
Invariant property
Feedforward control
Input-shaping
Disturbance input

ABSTRACT

In SOFCs, transient control of fuel utilization is achievable via input-shaping. In this paper, the approach is generalized to a feedforward control problem for second-order LTI systems with two inputs and one output. One is a measurable, time-varying, exogenous input and the other is a control input. The problem studied is exact tracking of a constant reference using the plant's DC gain vector. The problem considers plant models that can be divided into known and unknown parts, and where feedback is unavailable. Although SOFCs have nonlinear dynamics, the linear abstraction nevertheless helps predict the observed effectiveness of input-shaping.

1. Introduction

Amongst different types of fuel cells, SOFCs offer advantages including fuel flexibility and high tolerance to impurities, (Larminie & Dicks, 2003; Li, 2006; Nehrir & Wang, 2009). However, disadvantages such as susceptibility to fuel starvation limits its range of applications. This deficiency is primarily due to comparatively slow dynamic response of fuel and air delivery devices, and is reflected in the transient response of a single variable, namely fuel utilization. Fuel utilization, U, is defined as the ratio of hydrogen consumption to the net available hydrogen at the anode of an SOFC. Although high utilization implies high efficiency, very high utilization increases the susceptibility of SOFCs to fuel starvation, causing irreversible damages through drastic voltage drop and anode oxidation (Mueller, Brouwer, Jabbari, & Samuelsen, 2006). A target steady-state U set around 80–90% ensures optimal performance, (Campanari, 2001; Lazzaretto, Toffolo, & Zanon, 2004). Constant fuel utilization is a primary mode of operation of SOFCs (Gaynor, Mueller, Jabbari, & Brouwer, 2008; Nehrir & Wang, 2009). In this mode, the fuel flow is manipulated based on a steady-state relationship between U, fuel flow, and current (Mueller et al., 2006). In Slippey, Madani, Nishtala, and Das (2015), a generalized analytical study of this relationship reveals its invariance with respect to operating conditions such as temperature, pressure and rates of reforming reactions. It can be derived under partial knowledge of the plant, for reformer based SOFCs operating with a class of hydrocarbon fuels. Hence it is termed an *invariant property*, and fundamentally the invariance is due to certain conserved variables that define U.

While the aforementioned invariant property can be used to maintain a target U at steady-state, fuel starvation can still occur during power fluctuations. Cumulatively, such periods of fuel starvation can cause irreversible damage to the fuel cell. In Allag and Das (2012) and Das and Snyder (2013), it is shown that this can be prevented if the associated transient fluctuations in U are sufficiently attenuated. However, it is challenging to address this task through feedback since direct measurement or model-based estimation of U are relatively difficult. Direct measurement is difficult because U is a function of internal flow rates and concentrations of several species at multiple locations, leading to expensive and intrusive sensing. If sensed, the values may be unreliable due to rapidly changing composition of the gas mixture. Nonlinear observers provide a feasible alternative with lesser sensing requirement, (Abeysiriwardena & Das, 2016), although with associated computational requirements and model dependence. In contrast, despite being simply a DC gain, the invariant property can still be used for effective transient control of U (Allag & Das, 2012; Das & Snyder, 2013). To do so, the fuel flow rate which experiences lags, is treated as a measurable exogenous input whose influence on transient U is attenuated by *shaping* the control input, namely the current draw. This amounts to feedforward

* Corresponding author.
E-mail address: tuhin.das@ucf.edu (T. Das).

http://dx.doi.org/10.1016/j.conengprac.2016.08.008
0967-0661/

based transient control without augmented feedback. While this approach offers significant attenuation of transient U, a complete cancellation is not achieved. Nevertheless, the method's simplicity outweighs the issue of residual fluctuations in U.

It is noted that feedforward for SOFC systems appears in works such as (Carre et al., 2015; Mueller, Jabbari, Gaynor, & Brouwer, 2007; Oh, Sun, Dobbs, & King, 2014). In these works, the use of feedforward is to attain desired static operating points. In contrast, this paper focuses on using feedforward to influence the dynamical behavior of U in SOFCs, in addition to ensuring desired operating points. Thus, a broader sense of feedforward control is of interest in this paper. To this end, the above outlined transient problem is generalized to a special case of feedforward control (see Clayton, Tien, Leang, Zou, & Devasia, 2009; Franklin, Powell, & Emami-Naeini, 2014 and references therein) for second order systems with two inputs and one output. Some distinguishing features of the proposed feedforward problem are: (1) tracking of constant reference is considered, since U must be maintained at a constant target value; (2) feedback is assumed unavailable; (3) the plant model is assumed to contain unknown components that the feedforward control must be independent of; (4) of the two inputs, one is a measurable exogenous input and the other is treated as the control input. For multivariable LTI systems satisfying these features, the paper derives analytical conditions when exact transient control is feasible. For nonlinear and/or linear time-varying systems these conditions can help predict how effectively transient control is achievable. Simulation data shows how these conditions are roughly met by the fuel cell system, and consequently yield acceptable transient control of U even though the SOFC system is nonlinear and time-varying. This paper has similarities to the work in Madani and Das (2013) by the same authors. However, the unique contributions of this paper are: (1) a theorem that gives conditions under which the proposed approach is viable when the plant model has unknown components; (2) quantitative validation of the analytical results for the SOFC system.

2. Background

2.1. SOFC system and the invariant property

Consider a tubular SOFC which has three major components i.e. the steam reformer, the fuel cell stack and the combustor. The fuel is Methane, supplied with a molar flow rate of $\dot{N}_f$. The system is illustrated in Fig. 1. The reformer produces a hydrogen-rich gas which is supplied to the anode of the fuel cell. Electrochemical reactions occurring at the anode due to current draw results in a steam-rich gas mixture at its exit. A known fraction k of the anode exhaust is recirculated through the reformer into a mixing chamber where fuel is added. The steam reforming process occurring in the reformer catalyst bed is an endothermic process. The energy required to sustain the process is supplied from two sources, namely, the combustor exhaust that is passed through the reformer, and the aforementioned recirculated anode flow, as shown in Fig. 1. The remaining anode exhaust is mixed with the cathode exhaust in the combustion chamber. The combustor also serves to preheat the cathode air which has a molar flow rate of $\dot{N}_{air}$. Details are presented in Das, Narayanan, & Mukherjee (2010). Fuel utilization U for this system, which represents the ratio of fuel used by the anode for generating electricity to the amount supplied, is mathematically defined as (Campanari, 2001; Lazzaretto et al., 2004; Mueller et al., 2006):

$$U \triangleq 1 - \frac{\dot{N}_o\left(4\mathcal{X}_{1,a} + \mathcal{X}_{2,a} + \mathcal{X}_{4,a}\right)}{\dot{N}_{in}\left(4\mathcal{X}_{1,r} + \mathcal{X}_{2,r} + \mathcal{X}_{4,r}\right)} \tag{1}$$

where, $\mathcal{X}_{1,a}$, $\mathcal{X}_{2,a}$, $\mathcal{X}_{4,a}$ and $\mathcal{X}_{1,r}$, $\mathcal{X}_{2,r}$, $\mathcal{X}_{4,r}$ are the molar concentrations of CH_4, CO and H_2 in the anode and the reformer respectively and the flow rates $\dot{N}_o$ and $\dot{N}_{in}$ are shown in Fig. 1. The path followed by the fuel is indicated by lines marked red. The molar balance equations of individual species, along this path, in the reformer and anode are:

$$\begin{aligned}
N_r\dot{\mathcal{X}}_{1,r} &= k\dot{N}_o\mathcal{X}_{1,a} - \dot{N}_{in}\mathcal{X}_{1,r} + \mathcal{R}_{1,r} + \dot{N}_f \quad N_a\dot{\mathcal{X}}_{1,a}\\
&= \dot{N}_{in}\mathcal{X}_{1,r} - \dot{N}_o\mathcal{X}_{1,a} + \mathcal{R}_{1,a}N_r\dot{\mathcal{X}}_{2,r}\\
&= k\dot{N}_o\mathcal{X}_{2,a} - \dot{N}_{in}\mathcal{X}_{2,r} + \mathcal{R}_{2,r} \quad N_a\dot{\mathcal{X}}_{2,a}\\
&= \dot{N}_{in}\mathcal{X}_{2,r} - \dot{N}_o\mathcal{X}_{2,a} + \mathcal{R}_{2,a}N_r\dot{\mathcal{X}}_{3,r}\\
&= k\dot{N}_o\mathcal{X}_{3,a} - \dot{N}_{in}\mathcal{X}_{3,r} - \mathcal{R}_{1,r} - \mathcal{R}_{2,r} \quad N_a\dot{\mathcal{X}}_{3,a}\\
&= \dot{N}_{in}\mathcal{X}_{3,r} - \dot{N}_o\mathcal{X}_{3,a} - \mathcal{R}_{1,a} - \mathcal{R}_{2,a}N_r\dot{\mathcal{X}}_{4,r}\\
&= k\dot{N}_o\mathcal{X}_{4,a} - \dot{N}_{in}\mathcal{X}_{4,r} - 4\mathcal{R}_{1,r} - \mathcal{R}_{2,r} \quad N_a\dot{\mathcal{X}}_{4,a}\\
&= \dot{N}_{in}\mathcal{X}_{4,r} - \dot{N}_o\mathcal{X}_{4,a} - 4\mathcal{R}_{1,a} - \mathcal{R}_{2,a} - r_eN_r\dot{\mathcal{X}}_{5,r}\\
&= k\dot{N}_o\mathcal{X}_{5,a} - \dot{N}_{in}\mathcal{X}_{5,r} + 2\mathcal{R}_{1,r} + \mathcal{R}_{2,r} \quad N_a\dot{\mathcal{X}}_{5,a}\\
&= \dot{N}_{in}\mathcal{X}_{5,r} - \dot{N}_o\mathcal{X}_{5,a} + 2\mathcal{R}_{1,a} + \mathcal{R}_{2,a} + r_e
\end{aligned} \tag{2}$$

and the electrochemical reaction rate r_e is

$$r_e = i_{fc}\mathcal{N}_{cell}/nF. \tag{3}$$

In Eq. (2), $\mathcal{X}_{i,r}$ and $\mathcal{X}_{i,a}$ are the molar concentrations of species in the reformer and anode respectively, with $i = 1, 2, \ldots, 5$ representing CH_4, CO, CO_2, H_2 and H_2O in that order. N_r and N_a are the molar contents of the reformer and the anode, and k is the constant recirculation fraction shown in Fig. 1. $\mathcal{R}_{1,r}$, $\mathcal{R}_{2,r}$ and $\mathcal{R}_{1,a}$, $\mathcal{R}_{2,a}$ are the rates of formation of CH_4 and CO in the reformer and anode respectively. In Eq. (2), i_{fc} is the fuel cell current, $\mathcal{N}_{cell}$ is the number of series-connected cells, n=2 is the number of electrons participating in an electrochemical reaction, and F=96,485.34 Coul./mole is Faraday's constant. Further details about the equations can be found in Das et al. (2010). From Eqs. (1) and (2), the steady-state utilization U_{ss} is obtained as

$$U_{ss} = (1-k)/\left[\left(4nF\dot{N}_f/i_{fc}\mathcal{N}_{cell}\right) - k\right]. \tag{4}$$

Eq. (4) is independent of the reaction rates $\mathcal{R}_{1,r}$, $\mathcal{R}_{2,r}$, $\mathcal{R}_{1,a}$, $\mathcal{R}_{2,a}$ and the flow rates $\dot{N}_{in}$, $\dot{N}_o$. It is also invariant with respect to operating temperature, operating pressure, mass of reforming catalyst, and operating Steam-to-Carbon ratio (Das et al., 2010). Thus, Eq. (4) represents *an invariant relationship* between steady-state fuel utilization U_{ss} and the inputs, namely, fuel cell current i_{fc}, and fuel flow rate $\dot{N}_f$. Given a target U_{ss}, it can be used to determine $\dot{N}_f$ if i_{fc} is known and vice-versa. The invariance, specifically with respect to the reaction rates $\mathcal{R}_{1,r}$, $\mathcal{R}_{2,r}$, $\mathcal{R}_{1,a}$, $\mathcal{R}_{2,a}$, was shown to be valid for a wide range of hydrocarbon fuels and for multiple reformer types (Slippey et al., 2015). The work showed the invariance to exist for intrinsically conserved variables. To further understand the reason for invariance, a system-theoretic approach will be adopted in Section 3 of this paper.

2.2. Transient control of U through feedforward

The invariant property can be used to maintain constant utilization at steady-state, as depicted in Fig. 2(a). However, fuel starvation must be prevented even during transients. Typically, U must be around an optimal value ($\approx$85%) within narrow limits ($\pm$5%) even under significant power fluctuations. The limitations of using Eq. (4) alone without regulating the fuel cell current is demonstrated in Fig. 2(b)–(e). Here, step changes in power demand, $i_{fc,d}$, are directly translated to step changes in i_{fc}, Fig. 2(b). However, while the fuel demand $\dot{N}_{f,d}$ is based on Eq. (4), i.e.

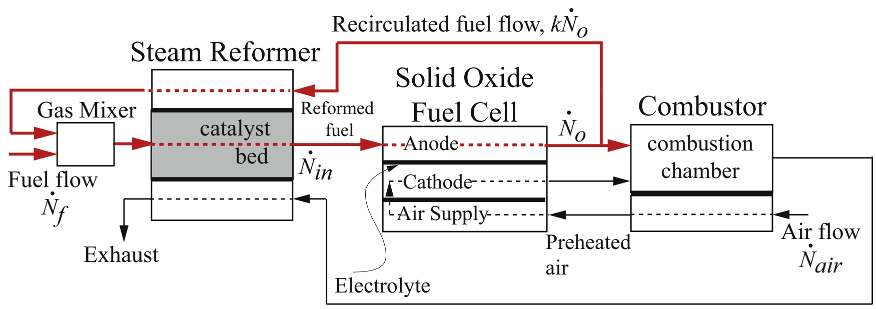

Fig. 1. Schematic diagram of SOFC system highlighting the flow path of interest.

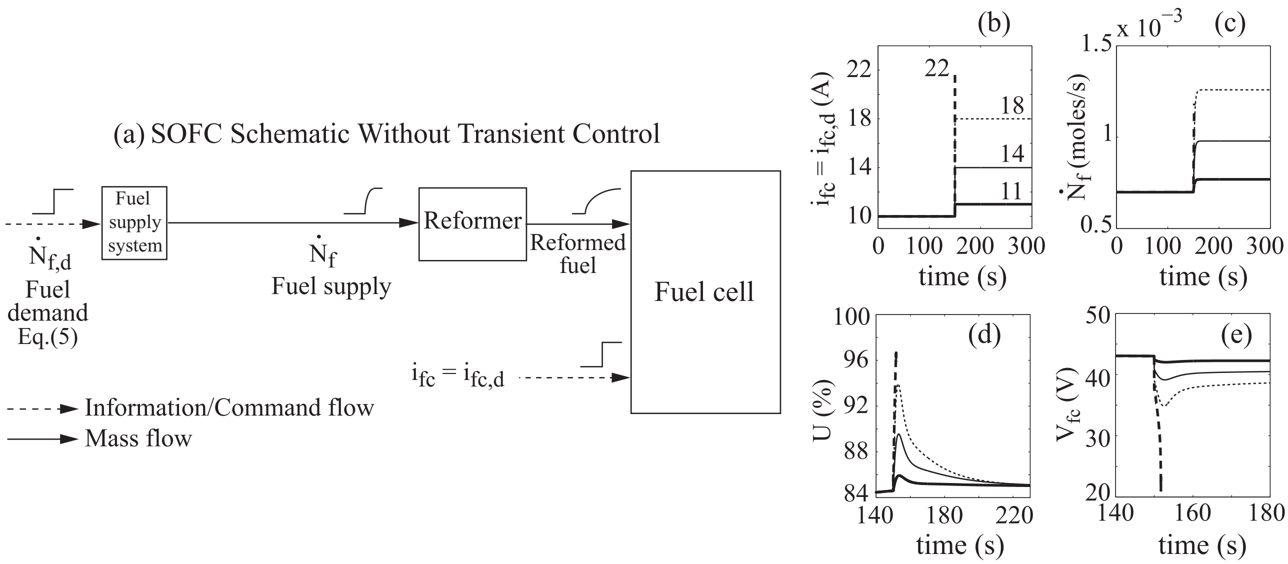

Fig. 2. SOFC system response in the absence of transient control of U, Allag and Das (2012).

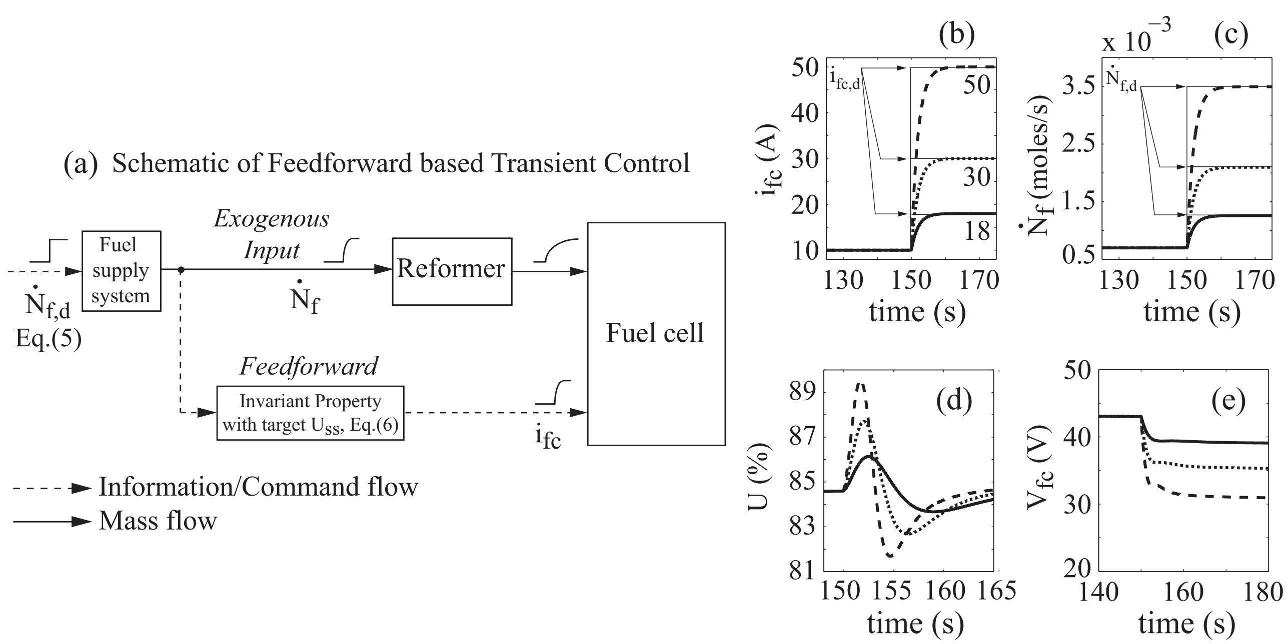

Fig. 3. SOFC system response with feedforward based transient control of U, Allag and Das (2012).

$$\dot{N}_{f,d} = i_{fc,d} N_{cell}[1 - (1 - U_{ss})k]/4nFU_{ss}, \tag{5}$$

the actual fuel flow $\dot{N}_f$ follows a transient determined by the dynamics of the Fuel Supply System (FSS), Fig. 2(c).

The results depict significant and prolonged transient departures from target $U_{ss} = 85\%$, even for small step changes in current from an original value of 10 A. Hydrogen starvation occurs with a step-change to $i_{fc,d} = 22$ A, and is manifested by $U \rightarrow 100\%$

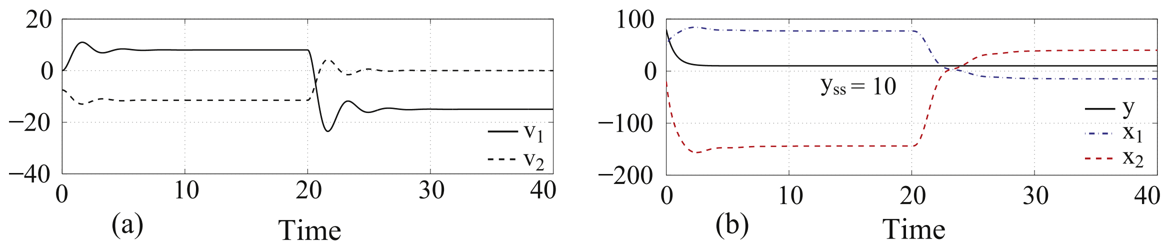

Fig. 4. Simulation showing isolation of y from exogenous input v_1 during transients.

and a complete voltage-loss, as shown in Figs. 2(d) and (e) respectively. To address this issue, i_{fc} is shaped based on $\dot{N}_f$ using feedforward, as shown in Fig. 3(a). This is achieved by continually updating i_{fc} using Eq. (4), based on the instantaneous fuel flow $\dot{N}_f$ and a target utilization U_{ss}, i.e.

$$i_{fc} = \dot{N}_f / \left[N_{cell}[1 - (1 - U_{ss})k]/4nFU_{ss} \right]. \tag{6}$$

Simulations presented in Fig. 3(b)–(e) depict the SOFC system's response to various step changes in $i_{fc,d}$. Fig. 3(d) shows a significant attenuation in the fluctuations of U compared to Fig. 2(d). Here $\dot{N}_f$ is treated as a measurable exogenous input whose influence on U is attenuated by the shaping of i_{fc}. Note that the proposed transient control allows significantly larger step changes in current without risking fuel starvation, Fig. 3(d), or voltage loss, Fig. 3(e) (a step change to $i_{fc,d} = 50$ A produces $< \pm 5\%$ fluctuation in U).

In the next section, this discussion will be generalized to a feedforward control problem for second-order LTI systems. The analysis is motivated by the following state-space formulation. Note that U in Eq. (1) can be expressed as

$$U = 1 - (\dot{N}_o(t) Z_2)/(\dot{N}_{in}(t) Z_1). \tag{7}$$

where,

$$Z_1 = \left(4X_{1,r} + X_{2,r} + X_{4,r}\right), \quad Z_2 = \left(4X_{1,a} + X_{2,a} + X_{4,a}\right). \tag{8}$$

From Eq. (2), the state equations of Z_1 and Z_2 can be written as:

$$\mathbf{M}\dot{\mathbf{z}} = \mathbf{A}\mathbf{N}(t)\mathbf{z} + \mathbf{B}\mathbf{u}, \quad \text{where}$$
$$\mathbf{z} = \begin{bmatrix} Z_1 \\ Z_2 \end{bmatrix}, \quad \mathbf{M} = \begin{bmatrix} N_r & 0 \\ 0 & N_a \end{bmatrix},$$
$$\mathbf{A} = \begin{bmatrix} -1 & k \\ 1 & -1 \end{bmatrix}, \quad \mathbf{N} = \begin{bmatrix} \dot{N}_{in}(t) & 0 \\ 0 & \dot{N}_o(t) \end{bmatrix}, \quad \mathbf{B} = \begin{bmatrix} 4 & 0 \\ 0 & -\frac{N_{cell}}{nF} \end{bmatrix},$$
$$\mathbf{u} = \begin{bmatrix} \dot{N}_f \\ i_{fc} \end{bmatrix}. \tag{9}$$

and the output $y = U$ can be expressed as,

$$y = U = (\mathbf{C}_1 \mathbf{N}(t)\mathbf{z})/(\mathbf{C}_2 \mathbf{N}(t)\mathbf{z}), \quad \mathbf{C}_1 = [1 \quad -1], \quad \mathbf{C}_2 = [1 \quad 0]. \tag{10}$$

In the above system definition, $\mathbf{N}(t)$ is time-varying and unknown, and it reaches unknown constant values at steady-states. Matrix $\mathbf{M}$ is unknown but assumed constant because the SOFC's operating pressure and temperature both involve small changes. The matrices $\mathbf{A}$, $\mathbf{B}$, $\mathbf{C}_1$ and $\mathbf{C}_2$ are all constant and known. Thus the system is linear and time-varying, it has a nonlinear output, and it consists of known and unknown components. The transient control problem can be formulated as follows: *given that the measurement of $\dot{N}_f(t)$ is available but there is no availability of feedback, and assuming $\mathbf{N}(t)$ and $\mathbf{M}$ to be unknown, determine $i_{fc}(t)$ that will attenuate fluctuations in U from U_{ss}.*

3. Generalization to a feedforward control problem

From the above outlined transient control problem of solid oxide fuel cells, a generalized transient control problem can be formulated and analyzed for second order LTI systems with 2-inputs and one output. Consider the following LTI system:

$$\dot{X} = AX + BV, \quad y = CX, \quad X = [x_1 \quad x_2]^T, \quad V = [v_1 \quad v_2]^T \tag{11}$$

where $A \in \mathbb{R}^{2\times2}$, $B \in \mathbb{R}^{2\times2}$, $C \in \mathbb{R}^{1\times2}$. Also let $V \in \mathbb{R}^{2\times1}$ represent the vector containing the control input and exogenous input. Either v_1 or v_2 can be treated as the exogenous input and the other as the control input. From Eq. (11), the steady-state input/output relation is therefore,

$$\dot{X}_{ss} = 0 \Rightarrow X_{ss} = -A^{-1}BV_{ss} \Rightarrow y_{ss} = -CA^{-1}BV_{ss}. \tag{12}$$

Next, the following conditions are imposed that will help define the specific feedforward problem that serves as a generalization of the transient control problem:

1. B and C matrices are known but A is unknown.
2. B is invertible.
3. The steady-state equation: $y = QV = [q_1 \; q_2]V = -CA^{-1}B\,V$, is known and $q_1, q_2 \neq 0$. Note that the knowledge of Q, the DC gain vector, does not imply a knowledge of A.
4. State feedback and output feedback are unavailable, but the exogenous input is measurable.

The following question is posed, as the exogenous input (say $v_1(t)$ without any loss of generality) varies, can $v_2(t)$ be designed under the conditions imposed above, such that $\lim_{t\to\infty} y(t) = y_{ss} = \delta$ where δ is a desired/target value? To this end, the following theorem is stated:

Theorem 1. *Consider the LTI system given in Eq . (11) for which all the above assumptions (1) – (4) are valid. If y is such that $CA^{-1} = \alpha C$, $\alpha < 0$, then with $\delta = QV = -CA^{-1}B\,V$, $\lim_{t\to\infty} y(t) = \delta$ for any transient in the exogenous input.*

Proof. First, observe that since C, B and $CA^{-1}B$ are known and B is invertible, CA^{-1} can be determined. Note that $C = \alpha CA$ implies $C\left(\frac{1}{\alpha}I - A\right) = 0$, and hence $1/\alpha$ is an eigenvalue of A with C being the corresponding eigenvector. Taking the time derivative of y yieldswhich implies that by choosing V to satisfy $CBV = -\frac{\delta}{\alpha}$, yields $\lim_{t\to\infty} y(t) = \delta$. Since $CA^{-1} = \alpha C$, by choosing V to satisfy

$$-CA^{-1}BV = QV = \delta \tag{14}$$

$\lim_{t\to\infty} y(t) = \delta$ is ensured.□

To illustrate the effectiveness of Theorem 1, a simulation result is shown in Fig. 4. The system chosen for the result in Fig. 4(a) and (b) is

$$A = \begin{bmatrix} 1 & 0.75 \\ -5 & -3 \end{bmatrix}, \quad B = \begin{bmatrix} 1 & -2 \\ -3 & 2 \end{bmatrix}, \quad C = \begin{bmatrix} 2 & 1 \end{bmatrix} \tag{15}$$

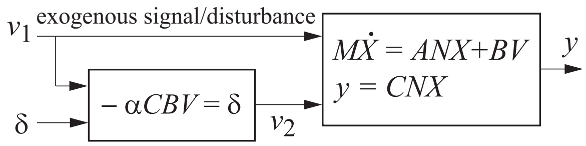

Fig. 5. Schematic of feedforward control. Exact transient control occurs when $CA^{-1} = \alpha C$, $\alpha < 0$. Figure represents Theorem 1 when $M = N = I_{2\times 2}$. When $M = \gamma N$, $\gamma > 0$, Theorem 2 is represented.

in which $V = [v_1\ v_2]^T$, v_1 is considered an exogenous input, and v_2 is the control input. The matrices B, C and $CA^{-1}B = -Q = [2/3\ 4/3]$ are assumed known. A is assumed unknown. It can be verified that B is invertible. Using B and $CA^{-1}B$, it can be verified that $CA^{-1} = -(2/3)C$, implying $\alpha = -2/3$. The target y is set to $\delta = 10$. This implies from Eq. (14) that if V satisfies $-CA^{-1}B\ V = -[2/3\quad 4/3]\left[v_1\ v_2\right]^T = 10$, i.e., if v_2 is designed as $v_2 = -0.5v_1 - 7.5$, then $\lim_{t\to\infty} y(t) = 10$. This is confirmed in Fig. 4(b).

In this simulation, the initial values $X(0) = \left[50\quad -20\right]^T$ were chosen arbitrarily. At t=20 s the disturbance v_1 was changed from 8 to -15 with an underdamped second order dynamics.

While Theorem 1 provides conditions under which ideal transient control of y can be achieved without using feedback and without a complete knowledge of A, it does not provide resolution on the known and unknown components of A. This is better addressed in Theorem 2, stated next, where the known and unknown components of the state-space system are structured according to that of the SOFC system in Eq. (9).

Theorem 2. *Consider the 2nd order LTI system*

$$M\dot{X} = ANX + BV, \quad y = CNX, \quad X = [x_1\quad x_2]^T, \quad V = [v_1\quad v_2]^T. \tag{16}$$

where $A \in \mathbb{R}^{2\times 2}$, $B \in \mathbb{R}^{2\times 2}$, and $C \in \mathbb{R}^{1\times 2}$, are known. The matrices $M \in \mathbb{R}^{2\times 2}$ and $N \in \mathbb{R}^{2\times 2}$ are unknown. Then, at steady-state $y = QV = [q_1\ q_2]^T V = -CA^{-1}BV$, and therefore the DC gain vector Q can be determined without the knowledge of M and N. Furthermore, if $q_1, q_2 \neq 0$, and $M = \gamma N$ with $\gamma > 0$, and

1. *if $CA^{-1} = \alpha C$, $\alpha < 0$, $\lim_{t\to\infty} y(t) = \delta$ can be achieved for any exogenous input $v_1(t)$ by applying the feedforward law*

$$\delta = QV = -CA^{-1}BV. \tag{17}$$

2. *If instead of (1), A is Hurwitz and γ is known, then $\lim_{t\to\infty} y(t) = \delta$ can be achieved for any exogenous input $v_1(t)$ by applying the feedforward law*

$$\delta = \left(QV + \frac{\gamma}{\alpha_2}CB\dot{V}\right), \tag{18}$$

where α_1 and α_2 are the coefficients of the characteristic equation of A, namely, $s^2 + \alpha_1 s + \alpha_2 = 0$.

Proof. Applying steady-state conditions to Eq. (16), observe that $y_{ss} = -CNN^{-1}A^{-1}B\ V_{ss} = -CA^{-1}B\ V_{ss}$. Thus the steady-state value of y is independent of M and N, which are unknown. Next, assume that the first condition above is satisfied. Then,

$$\dot{y} = CNM^{-1}ANX + CNM^{-1}BV = \frac{1}{\gamma}\left(CANX + CBV\right). \tag{19}$$

Since $CA^{-1} = \alpha C$, hence $CAN = (1/\alpha)CN$ and the above equation reduces to

$$\dot{y} = \frac{1}{\alpha\gamma}\left(y + CA^{-1}BV\right). \tag{20}$$

Since $1/\alpha\gamma < 0$, Eq. (20) is internally stable and the feedforward control of Eq. (17) will ensure $\lim_{t\to\infty} y(t) = \delta$ for any exogenous input $v_1(t)$.

Next assume that the second condition applies. Then,

$$\dot{y} = \frac{1}{\gamma}\left(CANX + CBV\right) \Rightarrow \ddot{y} = \frac{1}{\gamma^2}\left(CA^2NX + \gamma CB\dot{V} + CABV\right) \tag{21}$$

The Cayley–Hamilton theorem (Rugh, 1996) yields

$$s^2 + \alpha_1 s + \alpha_2 = 0 \Rightarrow A^2 + \alpha_1 A + \alpha_2 I = [0]$$
$$\Rightarrow \begin{cases} CA^2N = -\alpha_2 CN - \alpha_1 CAN \\ CAB = -\alpha_1 CB - \alpha_2 CA^{-1}B \end{cases} \tag{22}$$

Using Eqs. (21) and (22),

$$\gamma^2\ddot{y} + \alpha_1\gamma\dot{y} + \alpha_2 y = \alpha_1 CBV + \gamma CB\dot{V} + CABV = \alpha_2 QV + \gamma CB\dot{V}. \tag{23}$$

Since A is Hurwitz, $\alpha_1, \alpha_2 > 0$, and since $\gamma > 0$, the system is internally stable. Hence, applying the feedforward control of Eq. (18) ensures $\gamma^2\ddot{y} + \alpha_1\gamma\dot{y} + \alpha_2 y = \delta\alpha_2$, implying $\lim_{t\to\infty} y(t) = \delta$.□

A schematic of the feedforward control is given in Fig. 5. Finally, note that the systems in Eqs. (11) and (16) are *similarity transforms* of each other when $\gamma = 1$. Thus, a similarity transform not only preserves the DC gain vector, it also allows exact feedforward control when the mapping N is unknown.

4. Effectiveness of transient control in SOFC system

Returning to the SOFC system, note that while the structure of its state equation, Eq. (9), is similar to that in Eq. (16), the output equation, Eq. (10), is not. Despite this difference, since at steady-state, $\mathbf{N}(t)\mathbf{z} = \mathbf{N}_{ss}\mathbf{z}_{ss} = -\mathbf{A}^{-1}\mathbf{B}\mathbf{u}_{ss}$, the steady-state output takes the following convenient form:

$$y_{ss} = U_{ss} = \frac{\mathbf{C}_1\mathbf{A}^{-1}\mathbf{B}\mathbf{u}_{ss}}{\mathbf{C}_2\mathbf{A}^{-1}\mathbf{B}\mathbf{u}_{ss}}. \tag{24}$$

In Eq. (24), y_{ss} is related to $\mathbf{u}_{ss}$ through the known components only. Hence, for a desired y_{ss} and a measured/known exogenous input, the second input can be determined using Eq. (24). It can be verified by substituting $\mathbf{A}$, $\mathbf{B}$, $\mathbf{C}_1$ and $\mathbf{C}_2$ into Eq. (24) that the same expression as Eq. (4) is obtained. Note that transient control of y is achieved by implementing a feedforward strategy using Eq. (24), which is invariant with respect to $\mathbf{N}$ and $\mathbf{M}$. The strategy is

$$(\mathbf{C}_1 - y_{ss}\mathbf{C}_2)\mathbf{A}^{-1}\mathbf{B}\mathbf{u} = 0. \tag{25}$$

For the SOFC, $\mathbf{N}$ and $\mathbf{M}$ do not necessarily satisfy $\mathbf{M} = \gamma\mathbf{N}$ and $\mathbf{N}$ is time-varying. Hence an exact parallel of Theorem 2 is not applicable. However, transient control using Eq. (4) is quite effective as shown in Fig. 2, and its reason can be understood by drawing analogy from Theorem 2. Eq. (10) is differentiated with respect to time to obtain

$$\begin{aligned}\dot{y}\mathbf{C}_2\mathbf{N}\mathbf{z} &= \left(\mathbf{C}_1 - y\mathbf{C}_2\right)\mathbf{N}\dot{\mathbf{z}} + \left(\mathbf{C}_1 - y\mathbf{C}_2\right)\dot{\mathbf{N}}\mathbf{z} \\ &= \left(\mathbf{C}_1 - y\mathbf{C}_2\right)\mathbf{N}\mathbf{M}^{-1}\mathbf{A}\mathbf{N}\mathbf{z} + \left(\mathbf{C}_1 - y\mathbf{C}_2\right)\mathbf{N}\mathbf{M}^{-1}\mathbf{B}\mathbf{u} \\ &\quad + \left(\mathbf{C}_1 - y\mathbf{C}_2\right)\dot{\mathbf{N}}\mathbf{z}.\end{aligned} \tag{26}$$

Observe in Theorem 2, that the simplification of Eqs. (19) to (20) was possible because $CNM^{-1}AN$ was linearly dependent on CN. In the SOFC system, i.e. in Eq. (26), the term corresponding to $CNM^{-1}AN$ is $(\mathbf{C}_1 - y\mathbf{C}_2)\mathbf{N}\mathbf{M}^{-1}\mathbf{A}\mathbf{N}$. Using Eqs. (9) to (10), it simplifies to

Table 1
Directions of $(\mathbf{C}_1 - y\mathbf{C}_2)\mathbf{NM}^{-1}\mathbf{AN}$ vs. $\mathbf{C}_1\mathbf{N}$ in simulations.

Variables	Set 1	Set 2	Set 3
i_{fc} (A)	10	10	20
y_{ss} $(=U_{ss})$	0.6	0.85	0.85
N_a (moles)	46.4×10^{-3}	46.25×10^{-3}	45.3×10^{-3}
N_r (moles)	7.09×10^{-3}	7.4×10^{-3}	7.27×10^{-3}
$\dot{N}_o$ (moles/s)	5.62×10^{-3}	4.66×10^{-3}	9.33×10^{-3}
$\dot{N}_{in}$ (moles/s)	5.33×10^{-3}	4.36×10^{-3}	8.57×10^{-3}
$\mathbf{C}_1\mathbf{N} \times 10^3$	$[5.33 \;\; -5.62]$	$[4.36 \;\; -4.66]$	$[8.57 \;\; -9.33]$
$(\mathbf{C}_1 - y\mathbf{C}_2)\mathbf{NM}^{-1}\mathbf{AN} \times 10^3$	$[-2.25 \;\; 1.61]$	$[-0.82 \;\; 0.7]$	$[-3.28 \;\; 2.83]$
$\angle(\mathbf{C}_1 - y\mathbf{C}_2)\mathbf{NM}^{-1}\mathbf{AN} - \angle\mathbf{C}_1\mathbf{N}$	169.11°	173.27°	173.34°

$$(\mathbf{C}_1 - y\mathbf{C}_2)\mathbf{NM}^{-1}\mathbf{AN} = \left[-\frac{\dot{N}_{in}^2(1-y)}{N_r} - \frac{\dot{N}_{in}\dot{N}_o}{N_a} \quad \frac{k(1-y)\dot{N}_{in}\dot{N}_o}{N_r} + \frac{\dot{N}_o^2}{N_a} \right]. \tag{27}$$

Next note from Eqs. (8) and (10) that $\mathbf{C}_2\mathbf{Nz} = \dot{N}_{in}Z_1$ will always be positive. Hence in the output equation, i.e., $y\mathbf{C}_2\mathbf{Nz} = \mathbf{C}_1\mathbf{Nz}$, the term corresponding to CN is $\mathbf{C}_1\mathbf{N}$, which simplifies to

$$\mathbf{C}_1\mathbf{N} = \left[\dot{N}_{in} \quad -\dot{N}_o \right]. \tag{28}$$

Hence, the isolation of the exogenous input $\dot{N}_f$ through i_{fc} will be effective if there is an *approximate* linear dependence: $(\mathbf{C}_1 - y\mathbf{C}_2)\mathbf{NM}^{-1}\mathbf{AN} \approx \beta\mathbf{C}_1\mathbf{N}$, $\beta < 0$. This was verified to be true for several operating conditions for the SOFC system, some of which are tabulated below. The phase difference between these two vectors is close to 180° for many operating conditions. Note that the term containing $\dot{\mathbf{N}}$ in Eq. (26) provides additional perturbations in $y(t)$ and with its magnitude dependent on $\dot{N}_f$, which is non-zero during transience (Table 1).

5. Conclusion

The problem of attenuating transients in fuel utilization in SOFCs, arising from exogenous disturbances due to power fluctuations, was posed as a problem in feedforward control for second order dynamical systems. The problem was analytically studied for two-input single-output LTI systems. The results provide conditions under which the output variable can be completely isolated from measurable and time-varying disturbances using the plant's DC gain vector. The results assume an absence of feedback and presence of unknown components in the plant model. The invariant property that was employed for transient control in SOFCs, was generalized to the DC gain vector of the LTI system. Its invariance was attributed to the specific structure of the plant model that caused the DC gain to be independent of the aforementioned unknown components. Overall, the paper provides two simple theorems on feedforward control that are applicable to second order multivariable LTI systems. The theorems emerge from fuel cells where the corresponding dynamics are nonlinear and time-varying.

Acknowledgment

This work was supported by NSF Grant #1158845.

References

Abeysiriwardena, S., & Das, T. (2016). An adaptive observer for recirculation based solid oxide fuel cells. *ASME Journal of Dynamic Systems, Measurement, and Control*, *138*(1–11), 081004.
Allag, T., & Das, T. (2012). Robust nonlinear control of solid oxide fuel cell ultra-capacitor hybrid systems. *IEEE Transactions on Control Systems Technology*, *20* (1), 1–10.
Campanari, S. (2001). Thermodynamic model and parametric analysis of a tubular SOFC module. *Journal of Power Sources*, *92*(1–2), 26–34.
Carre, M., Brandenburger, R., Friede, W., Lapicque, F., Limbeck, U., & da Silva, P. (2015). Feed-forward control of a solid oxide fuel cell system with anode offgas recycle. *Journal of Power Sources*, *282*, 498–510.
Clayton, G. M., Tien, S., Leang, K. K., Zou, Q., & Devasia, S. (2009). A review of feedforward control approaches in nanopositioning for high-speed SPM. *Journal of Dynamic Systems, Measurement, and Control*, *131*(1–19), 061101.
Das, T., Narayanan, S., & Mukherjee, R. (2010). Steady-state and transient analysis of a steam-reformer based solid oxide fuel cell system. *ASME Journal of Fuel Cell Science and Technology* 7 (1) 011022–(1–10).
Das, T., & Snyder, S. (2013). Adaptive control of a solid oxide fuel cell ultra-capacitor hybrid system. *IEEE Transactions on Control Systems Technology*, *21*(2), 372–383.
Franklin, G. F., Powell, J. D., & Emami-Naeini, A. (2014). *Feedback control of dynamic systems* (7th ed.). Upper Saddle River, NJ: Pearson.
Gaynor, R., Mueller, F., Jabbari, F., & Brouwer, J. (2008). On control concepts to prevent fuel starvation in solid oxide fuel cells. *Journal of Power Sources*, *180*, 330–342.
Larminie, J., & Dicks, A. (2003). *Fuel cell systems explained* (2nd ed.). Chichester, West Sussex, England: John Wiley and Sons Ltd.
Lazzaretto, A., Toffolo, A., & Zanon, F. (2004). Parameter setting for a tubular SOFC simulation. *Journal of Energy Resources Technology*, *126*(1), 40–46.
Li, X. (2006). *Principles of fuel cells*. New York, NY: Taylor and Francis Group.
Madani, O., & Das, T. (2013). Transient control in multivariable systems: A study motivated by fuel cells, In *ASME dynamic systems and control conference*, Palo Alto, CA, October 21–23 (Vol. 1, p. V001T03A003).
Mueller, F., Brouwer, J., Jabbari, F., & Samuelsen, S. (2006). Dynamic simulation of an integrated solid oxide fuel cell system including current-based fuel flow control. *Journal of Fuel Cell Science and Technology*, *3*(2), 144–154.
Mueller, F., Jabbari, F., Gaynor, R., & Brouwer, J. (2007). Novel solid oxide fuel cell system controller for rapid load following. *Journal of Power Sources*, *172*, 308–323.
Nehrir, M. H., & Wang, C. (2009). *Modeling and control of fuel cells—Distributed generation applications*. Hoboken, NJ: John Wiley and Sons, Inc.
Oh, S., Sun, J., Dobbs, H., & King, J. (2014). Model predictive control for power and thermal management of an integrated solid oxide fuel cell and turbocharger system. *IEEE Transactions on Control Systems Technology*, *22*(3), 911–920.
Rugh, W. J. (1996). *Linear system theory* (2nd ed.). Upper Saddle River, NJ: Prentice-Hall.
Slippey, A., Madani, O., Nishtala, K., & Das, T. (2015). Invariant properties of solid oxide fuel cell systems with integrated reformers. *Energy*, *90*(1), 452–463.